Letter of Intent to PAC 51

The Axial Form Factor of the Nucleon from Weak Capture of Positrons

A medium energy polarized positron beam would enable the extraction of the axial form factor $G_A(Q^2)$ of the nucleon and its four-momentum transfer square (Q^2) dependence, using the weak capture reaction in deuterium ($\vec{e}^{+} + {}^2\mathrm{H} \rightarrow 2p + \bar{\nu}_e$). A polarized positron beam with beam energies between 2.0 - 6.0 GeV can be used for a cross section measurement and a clean measurement of the background utilizing parity violation in the weak capture process. In addition to the poorly known axial form factor it will be possible to extract the axial charge radius (r_A), the axial coupling constants (g_A), and the axial dipole mass (M_A). We propose an experiment using a setup similar to the Tagged Deep Inelastic Scattering experiment (TDIS)– a thin walled target cell inside a compact solenoidal magnet and a radial recoil detector to tag a pair of recoil protons. The proposed positron capture based measurement would have a completely different set of systematic uncertainties compared to all currently used methods and may help resolve several current discrepancies of the weak interaction parameters .

I. INTRODUCTION AND PHYSICS MOTIVATION

One of main goals of Quantum Chromodynamics (QCD) is to understand the nucleon in terms of the underlying quarks and the gluons which bind them. One of the remarkable features of the nucleon is its large mass compared to the small current masses of the quarks. It is supposed that the mechanism of spontaneous chiral symmetry breaking in QCD has a fundamental role in the large constituent mass of the quarks when bound inside the nucleon. One of the ways to study quarks bound inside nucleons is to measure their electroweak current. The vector part of this current is well measured via electron scattering experiments and constrained by charge conservation. Moreover, the contribution of up, down and strange quarks to the nucleon charge and magnetization distribution have been obtained from precise measurements of the nucleon electromagnetic form factors [1] and vector weak form factors [2]. They are found to be not particularly sensitive to the details of QCD as the vector currents are conserved for massive quarks [3]. On the other hand, the nucleon axial-vector current which is related to the spontaneously broken chiral symmetry and the axial anomaly is much more sensitive to the details of QCD [4], but it is not as well known. The nucleon matrix element of the axial current is expressed in terms of two form factors, the weak axial form factor of the nucleon, $G_A(Q^2)$, and the induced pseudoscalar form factor, $G_P(Q^2)$. Typically, these are not directly accessible in electron scattering and are measured in quasielastic neutrino scattering [5], low energy pion electroproduction experiments [6] and muon capture experiments [7]. They are measured at low momentum transfer and tend to have large uncertainties with very little information for $Q^2 > 1$ $(\mathrm{GeV/c})^2$ as shown in Fig. 1. Among these the $G_P(Q^2)$ is the least known. Thus, measuring $G_A(Q^2)$ and $G_P(Q^2)$ using new experimental methods is vital for a rigorous understanding of the nucleon's QCD structure.

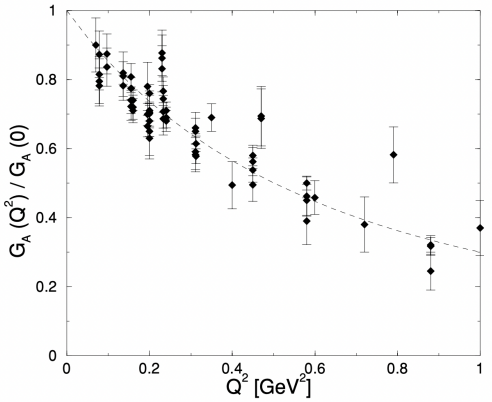

FIG. 1. Experimental data for the normalized axial form factor extracted from pion electroproduction experiments in the threshold region. Various theoretical models were used in the analysis to extract $G_A(Q^2)$. The dashed curve shows a dipole fit with an axial mass $M_A = 1.1$ GeV. Reproduced from Ref. [8].

Additionally, the axial charge or coupling, $g_A \equiv G_A(Q^2 = 0)$, and $< r_A^2 >= -\frac{6}{g_A}\frac{dG_A}{dQ^2}(Q^2 = 0)$ the axial charge radius, are fundamental weak interaction parameters. They are critical for description of weak interaction observables, such as neutrino-nucleon quasielastic scattering cross sections, muon capture rates, solar and reactor neutrino fluxes and neutrino oscillation experiments. They are also necessary input for the Goldberger-Treiman relation, the Bjorken sum rule, primordial nucleosynthesis and cosmic microwave background anisotropies [9, 10]. Usually g_A can be measured with high precision from neutron beta decay asymmetries. However, a number of anomalous and interconnected discrepancies have developed among the recent extractions of g_A and other weak interaction parameters, as discussed below.

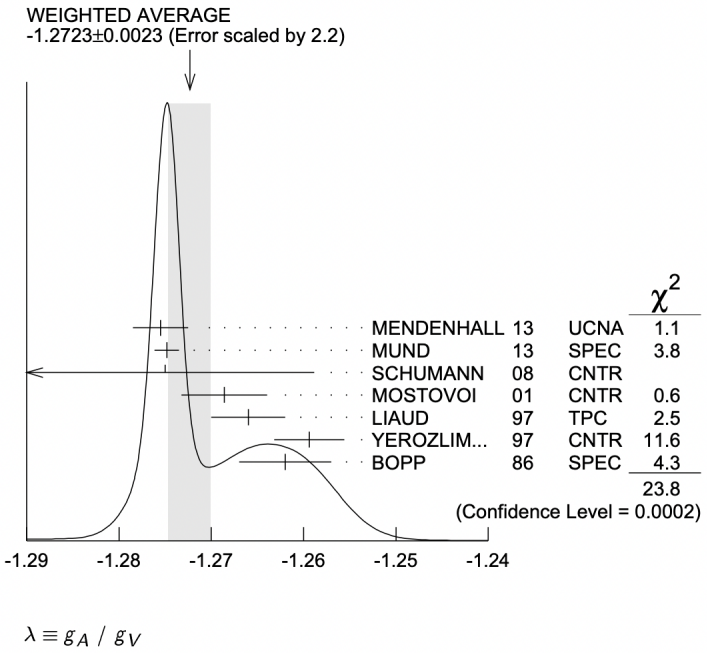

FIG. 2. The ratio of the weak coupling constant g_A and g_V obtained using the neutron beta decay asymmetry parameter A [11].

The relative strength of the axial to vector coupling constants, $\lambda = g_A/g_V$ are independently obtained from the β-decay correlation coefficients such as the beta-electron asymmetry correlation coefficient, A, and the neutrino-electron correlation coefficient, a. The values of λ obtained from β-decay correlation measurements have been summarized by Particle Data Group [11]. An anomalous 5σ difference between measurements before and after 2002 [12, 13] has been observed as see in Fig. 2. Moreover, λ obtained from the β-decay correlation coefficients, A and a, disagree with each other. Neglecting the four measurements from before 2002, which have larger than 10% systematic uncertainties [14], the averages of λ differ by 3 standard deviations and are thus incompatible.

Moreover, since the neutron lifetime, τ_n, is related to the values of λ and the CKM matrix parameter, V_{ud} [16, 17], this discrepancy in the measurement of λ has a direct implication [13] for the neutron lifetimes puzzle– the $>4\sigma$ difference in the neutron lifetime when measured using neutron beams vs trapped neutrons [18, 19]. Further muddying the waters, another related anomaly is the 4.4σ discrepancy between the values of V_{ud} obtained from two independent methods: from $0^+ \to 0^+$ super-allowed decays [11, 20], and via CKM-unitarity ($V_{ud}^2 + V_{us}^2 + V_{ub}^2 = 1$)[11]. A combination of the values of V_{ud} and λ that are consistent with the two values of neutron lifetime have been shown in Fig. 3, which demonstrates the current very puzzling status of the weak interaction parameters.

Finally, the neutrino charge current quasi-elastic cross section [21, 22] disagrees between different experiments (see Fig. 4), leading to a large discrepancy in the $< r_A^2 >$ and axial mass M_A extracted from these data, assuming the axial form factor has a simple dipole form. [23]. They suggest that the axial form factor obtained from recent global fits to neutrino scattering data have a much larger uncertainty than determined in the original analyses [5]. A recent review article [24] shows that the axial form factor obtained from different Lattice QCD (LQCD) calculations are consistent but collectively disagree with existing models and

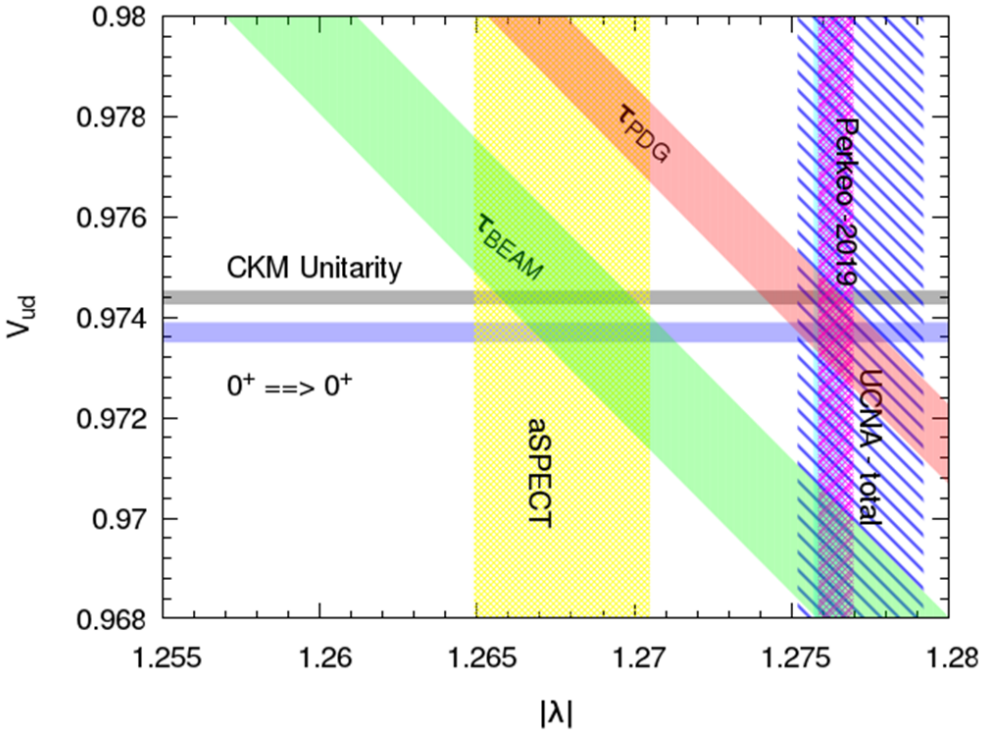

FIG. 3. The vertical axis shows the values of V_{ud} from global analysis of β-decay between $0^+ \to 0^+$ states (solid blue) and CKM unitarity (gray band). The horizontal axis show the λ extracted from the neutrino-electron correlation coefficient, a (aSPECT, yellow band) and various beta-electron asymmetry correlation coefficient, A (hatched bands). The diagonal bars are the neutron lifetime measurements using neutron beams (green band) and the PDG value which is dominated by neutron trap measurements. Figure credit N. Fomin [15].

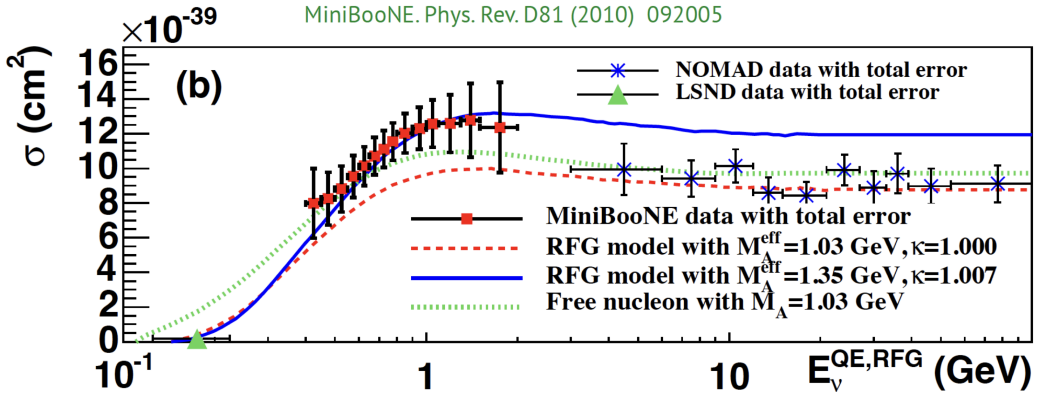

FIG. 4. The measured muon neutrino charge current quasi-elastic cross section as a function of the neutrino energy. The data are from the MiniBooNE collaboration [21] and the NOMAD collaboration [22]. The figure is reproduced from Ref. [23].

neutrino data as shown in Fig. 5. This has very large implications for current and future neutrino oscillation experiments [24]. Furthermore, it was recently reported that the axial form factor, $< r_A^2 >$ and axial mass M_A obtained from neutrino scattering on hydrogen and deuterium are incompatible with each other [25]. It is clear from all of this discussion that the current knowledge of the weak axial current is ripe for a new experimental method with completely different systematics to help resolve the numerous puzzles and anomalies.

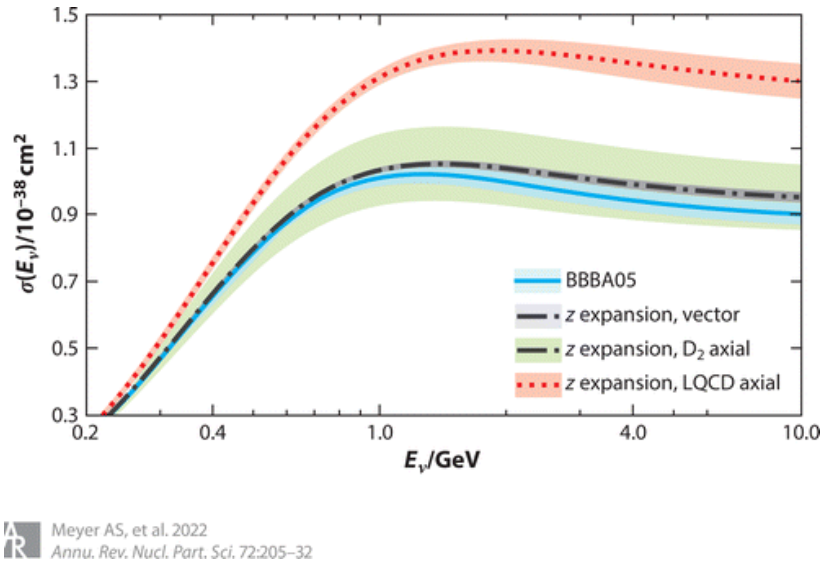

FIG. 5. The calculated neutrino cross-sections on a free neutron, with their uncertainty bands, for various choices of parameterization. The width of the upper red band, which comes from the LQCD results. The LQCD uncertainty is also noticeably smaller than the green band that arises from the deuterium scattering determination of $F_A(Q^2)$. The figure is reproduced from Ref. [24].

The weak capture of polarized positrons in deuterium– $\vec{e}^{+} + {}^2\mathrm{H} \rightarrow 2p + \bar{\nu}_e$, is well suited for this purpose. A polarized positron beam with beam energies between 2.0 - 6.0 GeV can be used to extract $G_A(Q^2)$ of the nucleon over a wide range of Q^2 using this capture process. The Q^2 dependence of $G_A(Q^2)$ will allow a more complete understanding of the nucleon in QCD. It can be used to extract the fundamental weak interaction parameters g_A and $< r_A^2 >$, which may help resolve a number of recent puzzles. It can also be used to search for right handed currents, second class currents [26] and meson-exchange currents [27]. Furthermore, the weak axial form factor should also be measured in light nuclei (^{3}He and ^{4}He) in order to confirm that the large value of the axial form factor of the proton is indeed a result of spontaneous symmetry breaking and not from some large current mass [28]. We describe a experimental program that will be capable of carrying out these measurements with a medium energy polarized positron beam at JLab.

II. POSITRON CAPTURE CROSS SECTION AND BACKGROUNDS

The capture process and its kinematics are shown in Fig. 6. Although the cross section for electron scattering decreases rapidly with increasing Q^2, the cross section for typical weak processes increases approximately linearly [29] with Q^2. For positrons of negative helicity the double differential cross section in the lab frame, for small relative momentum (< 10 MeV) between the final proton pair, is given by [29];

$$\frac{d^2\sigma}{dE_\nu d\Omega_\nu} = \frac{G^2 E_\nu^2 m_p |p_{rel}|}{8\pi^4} \int \frac{d\Omega_{rel}}{4\pi} \sum |M|^2 \tag{1}$$

where $G = G_F \cos\theta_C$, G_F is the Fermi constant and θ_C is the Cabibbo angle, m_p is the nucleon mass, p_{rel} is the relative momentum of the proton pair in the final state, the sum is over the final internal degrees of freedom and averaged over the initial states except for beam polarization, $|M|^2$ is a function of the vector and axial form factors, under nucleon only impulse approximation and the assumption that $m_\nu = 0$, the relative proton pair energy E_{rel} <10 MeV is small and neglecting the small positron mass. Note that the cross section for positive helicity positrons is strictly zero in this formalism. The cross section can be expressed as a function of the kinematic variables, positron beam energy, recoil neutrino energy and angle, E_e, E_ν and θ_ν. The E_ν and θ_ν of the undetected neutrino are determined from the momentum of the recoiling proton pair

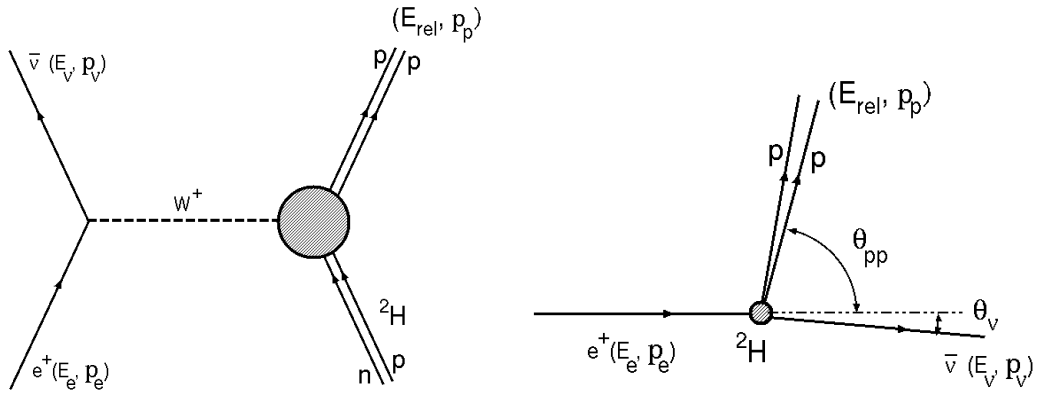

FIG. 6. (left) The weak capture process and (right) kinematics of the process with E_{rel} as the relative energy and p_p the momentum of the proton pair.

and hence the momentum transfer is given by $q = (p_e - p_p)$ [29]. The cross section can be further simplified to:

$$\frac{d\sigma}{dE_\nu} = \frac{G^2 m_p |p_{rel}|}{\pi} \frac{E_\nu}{E_e} \left[F_2(Q^2) \cos^2\theta_\nu + \left(2F_1(Q^2) + \frac{E_e + E_\nu}{m_p} F_3(Q^2) \right) \sin^2\theta_\nu \right], \tag{2}$$

where the form factors F_1, F_2 and F_3 are various combinations of G_A, and the electromagnetic form factors of the proton and neutron ,G_E and G_M. The cross section essentially depends on the axial form factor G_A and the difference between the neutron and proton electric ($G_E = G_E^n - G_E^p$) and magnetic ($G_M = G_M^n - G_M^p$) form factors. Using this formalism the cross section was calculated for 2, 4 and 6 GeV negative helicity positron beam by Mintz *et al.* [30] and W-Y. P. Hwang [29] (note that the cross section is zero for positive helicity positrons). Fig. 7 shows the cross sections as a function of the proton pair angle (left) and the neutrino angle (right) reproduced from the two calculations. As seen in Fig. 7 the cross section peaks for the proton pair being emitted essentially perpendicular to the beam and for very forward going neutrinos. Also note that the cross section increases with positron beam energy. The contribution to the capture cross section from the G_A, G_V and G_M form factors are shown in Fig. 8 for $E_{e^+} = 2$ GeV. Here G_V is the form factor of the vector current matrix element. It is clear that the axial form factor is the largest contribution to the cross section. Moreover, since G_V and G_M are well known from electron scattering experiments, the axial form factor G_A could be measured at fixed Q^2 by varying the positron beam energy and the angle of the recoil proton pair.

The kinematics of the positron capture reaction shown in Fig. 9 for 2, 6 and 11 GeV positrons. A recoil proton detector for the proton pairs with momentum between 100 - 500 MeV/c emitted at large angle (70 - 90 deg) will cover a Q^2 range of 0.01 - 0.5 GeV^2 with large overlap between the different beam energies. This will allow the axial form factor G_A to be measured at fixed Q^2 by varying the positron beam energy and the angle of the recoil proton pair.

The main source of background is quasi-elastic single nucleon knockout from the deuteron. The kinematics of the quasi-elastic scattering are essentially identical to the kinematics of the capture process (as shown in Fig. 10) and typically the cross section of quasi-elastic scattering is nine orders or magnitude higher than the weak capture process. The largest background comes from the accidental coincidence of two quasi-elastically scattered protons. The next largest background is from quasi-elastic neutron knockout from the deuteron followed by neutron to proton charge exchange rescattering. For this second largest background the parallel kinematics of the quasi-elastic scattering and the two step rescattering process needed to produce the pair of protons with small relative momentum between them will reduce the effective background cross section by at least an order of magnitude [31] compared to the accidental coincident background (the largest background).

We will use two key strategies to suppress the background; i) the scattered positron from the quasi-elastic process will be detected in anti-coincidence with the pair of coincident recoil protons which will allow a significant reduction of the background. ii) The large assymmetry from the difference between the positive helicity (zero capture cross section) and the negative helicity positrons will allow for suppression of the large background and isolation of the signal (this technique was first discussed in Ref. [32, 33]). Both of these strategies are discussed in detail in the next section. The requirement of detecting the scattered positrons

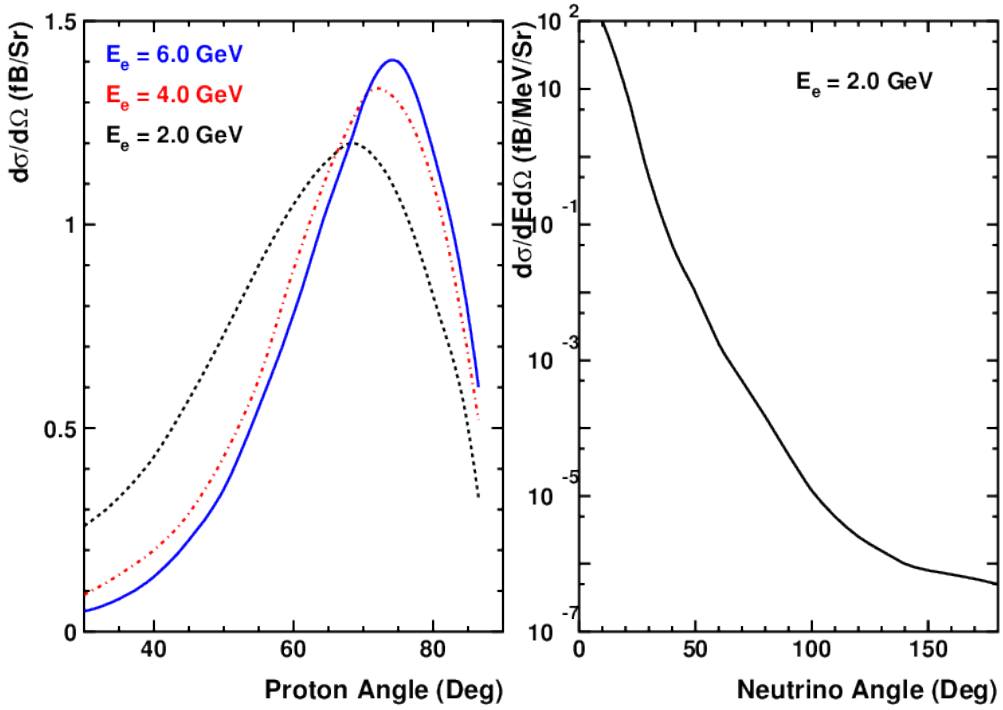

FIG. 7. (left) The differential cross section as a function of angle of proton pair for $E_{e^+} = 2$, 4 and 6 GeV from Mintz *et al.* [30]. (right) The differential cross section as a function of the neutrino emission angle for $E_{e^+} = 2$ GeV and $E_{rel} = 5$ MeV, from W-Y. P. Hwang [29].

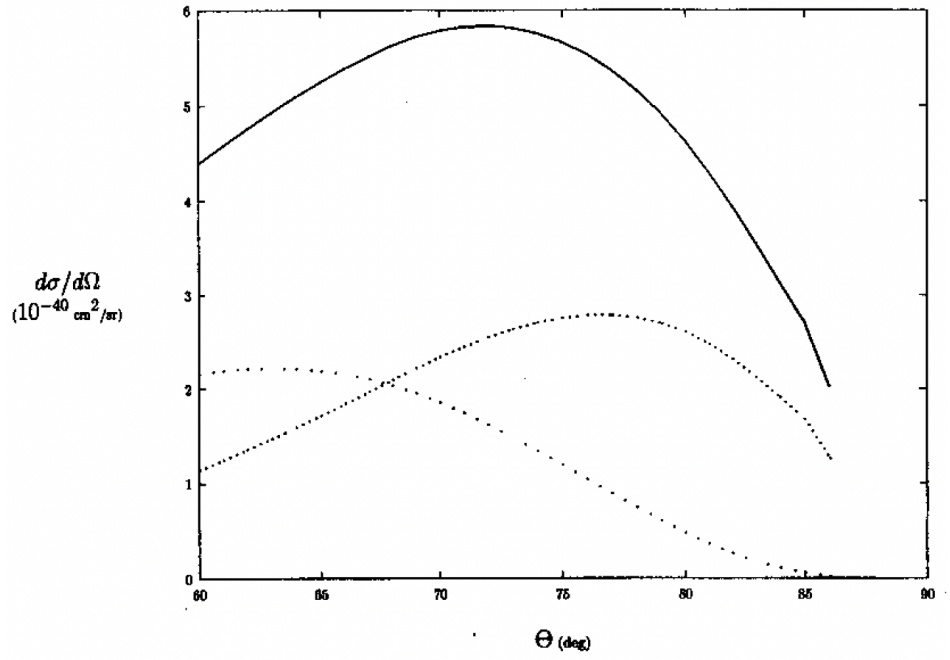

FIG. 8. The contributions from G_A (solid line), G_V (dense dotted line) and G_M (dotted line) to the differential cross section as a function of angle of proton pair for $E_{e^+} = 2$ GeV from Mintz *et al.* [30].

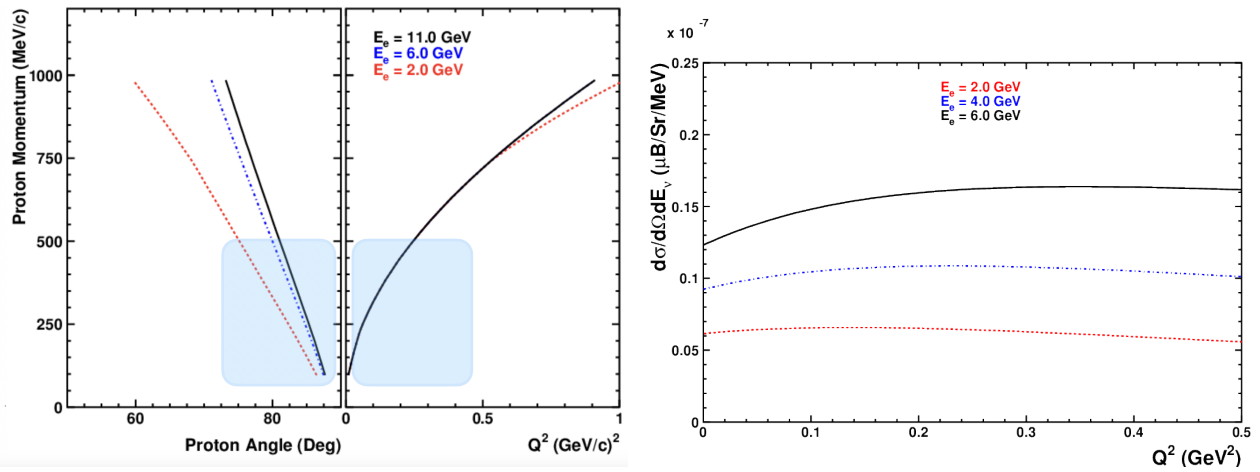

FIG. 9. (left) The momentum of the recoil protons vs their emission angle from the capture of 2 GeV (dashed), 6 GeV (dot-dashed) and 11 GeV (solid) positrons. (middle) The momentum of the recoil protons vs the four momentum transfer squared (Q^2) for the capture of 2 GeV (dashed), 6 GeV (dot-dashed) and 11 GeV (solid) positrons. The 6 and 11 GeV lines cannot be distinguished in this figure. The blue shaded region shows the kinematic range to be covered by the proposed experiment. (right) The capture cross section for 2 GeV (dashed), 6 GeV (dot-dashed) and 6 GeV (solid) positrons in the blue shaded region indicated in the kinematics plot.

from the quasi-elastic process in anti-coincidence is the main reason why the experiment is restricted to 2 – 6 GeV positrons although the cross section for the capture process increases with energy. For energies of higher than 6 GeV, the positrons from the quasi-elastic process in the desired Q^2 range, have scattering angles less than 5-degrees which cannot be detected in the standard spectrometers at JLab.

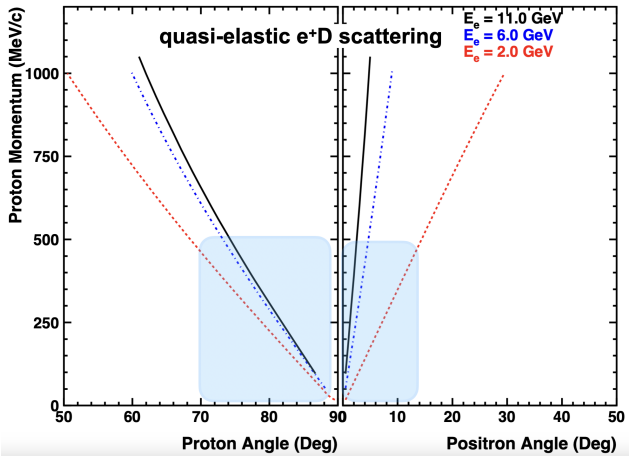

FIG. 10. (left) The momentum of the recoil protons vs their emission angle from the quasi-elastic positron-deuteron scattering of 2 GeV (dashed), 6 GeV (dot-dashed) and 11 GeV (solid) positrons. (right) The momentum of the recoil protons vs the positron scattering angle from the quasi-elastic positron-deuteron scattering of 2 GeV (dashed), 6 GeV (dot-dashed) and 11 GeV (solid) positrons. The blue shaded region shows the kinematic range to be covered by the proposed experiment. At 11 GeV the positron scattering angel is $< 5\ ^\circ$ and cannot be detected in the standard spectrometers.

III. THE EXPERIMENTAL SETUP

A 2 – 6 GeV positron beam with 60% polarization and beam current of 200 nA will be incident on a thin walled 40 cm ^{2}H gas target at 6 atm. pressure (similar to targets proposed for the TDIS and the ALERT experiments). The target will be radially surrounded by a recoil proton detector similar to the rTPC used in the BoNuS12 experiment [34], or the one being built for the ALERT [35] experiment or the mTPC proposed for the TDIS [36] experiment. Schematics of these detectors are shown in Fig. 10 and their key parameters are compared in Table I. The recoil detector will tag the pair of 100 - 500 MeV/c protons at large polar angles (70 - 90 deg) and 2π azimuthal angle. A solenoidal field around the target would help control the large charge particle load from Bhabha scattering. The thermal polarization of the target at room temperaturs is $\sim$ few ppm and should not be an issue for this experiment. We have used the TDIS mTPC as the recoil detector for all rate and performance estimates. The expected momentum resolution is $\Delta p/p = 0.5 - 5\%$ over the 100 – 500 MeV/c momentum range of the protons. This leads to a Q^2 resolution of $\Delta Q^2/Q^2 = 1 - 10\%$. This is based on the simulated performance of the mTPC for the TDIS experiment.

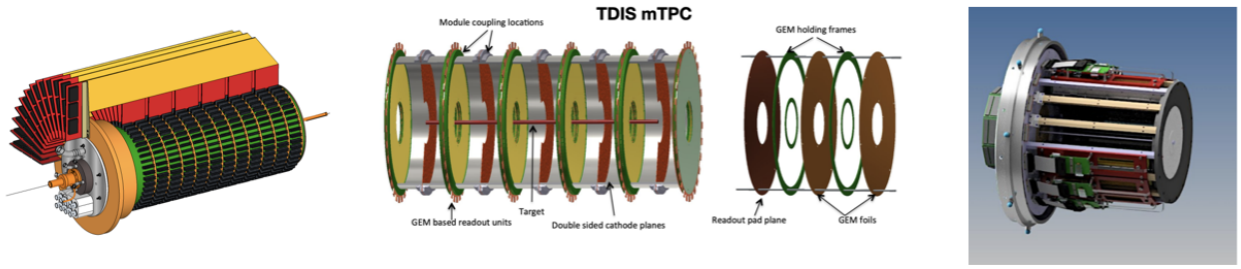

FIG. 11. Examples of recoil detectors that would be suitable for this experiment. The BoNuS12 rTPC (left) TDIS mTPC (middle) and the ALERT TPC (right).

Property	rTPC	mTPC	ALERT
length (cm)	40	40	35
momentum range (MeV/c)	70 - 250	7- - 500	70 - 250
momentum resolution (%)	10	0.5 - 5	10
	(for 100 MeV/c)	(for 70 - 500 MeV/c)	(for 100 MeV/c)
azimuthal coverage (deg)	360	360	340
z resolution (mm)	3	1	3

TABLE I. The properties of the BoNuS12 rTPC, the TDIS mTPC and the ALERT TPC.

In order to reduce the large background from quasi-elastic scattering, the scattered positrons have to be detected in time and vertex anti-coincidence with the pair of protons. This requires a positron spectrometer for small angle positron detection such as the super bigbite spectrometer (SBS), or the CLAS12 spectrometer (along with the forward tagger). A schematic using SBS is shown in Fig. 11 which is adapted from the setup of the TDIS experiment. Finally the positron polarization will be used to distinguish the capture process from the background since the capture process occurs only for negative helicity positrons.

The experiment will use a few different polarized positron beam energies from 2 - 6 GeV. The pair of protons from the capture process will be detected in coincidence over a range of angles (70 – 90 deg) at fixed Q^2. This will allow the extraction of $G_A(Q^2)$ over a range of Q^2, which will also allow for the extraction of $< r_A^2 >$ from the slope as a function of Q^2 extrapolated to $Q^2 = 0$ and the axial charge g_A by extrapolating $G_A(Q^2)$ to $Q^2 = 0$.

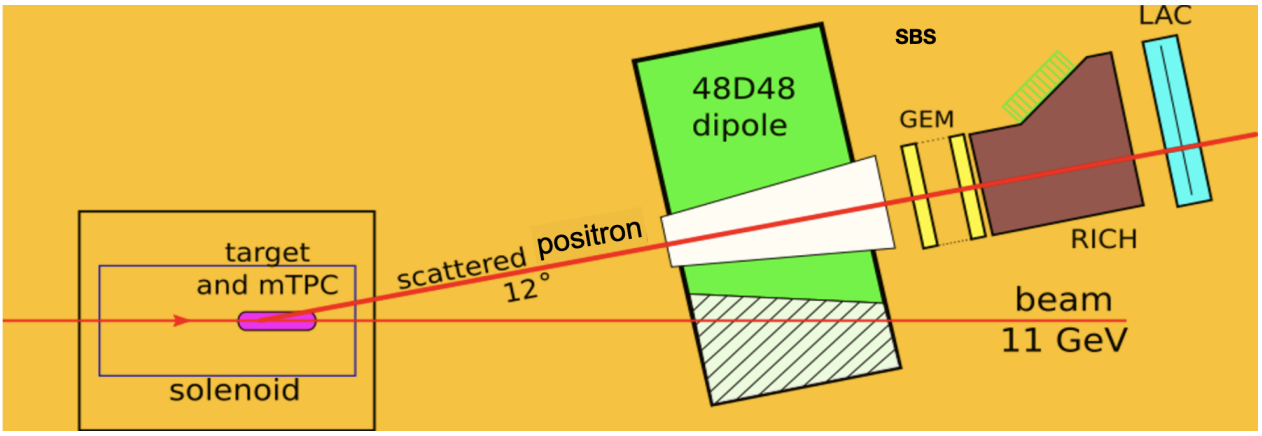

FIG. 12. The experimental setup, where the low energy large angle proton pair is detected in the mTPC recoil detector surrounding the thin walled target inside a solenoidal field. The background-producing forward going quasi-elastically scattered positrons are detected in time and vertex anti-coincidence by the SBS spectrometer. The polarization of the positron is used to separate the signal from the backgroud since the weak capture process is allowed only for negative helicity positrons.

IV. SIGNAL AND BACKGROUND RATES

We have estimated the signal rates for 2 – 6 GeV positrons with 60% polarization and 200 nA current incident on a 40 cm long and 6-atm pressure deuterium gas target, with a luminosity of 8×10^{34} cm^{-2}/s. The proton pair will be detected in coincidence, in a recoil detector with 2π azimuthal coverage, in 10-deg polar angle bins and 100 MeV/c proton momentum bins (corresponding to 30 MeV/c momentum bins for the undetected neutrino). The cross section for the weak capture of 4 GeV positrons is 1×10^{-9} μB/Sr/MeV cm^{2}sr^{-1}, which gives a count rate of 3×10^{-2}/s. For the 4 GeV positrons the cross section for the background quasi-elastic scattering process is 0.9 μB/Sr which is a factor of $\sim 10^9$ larger or a rate of $\sim3\times 10^7$/s. This implies that the two-proton accidental time and vertex coincidence rate, assuming a 20 ns coincidence window and a 2 mm vertex resolution, is; $R_{2p} = r_{prot1} \times r_{prot2} \times \tau \times (2.5\sigma_{z1}/L) \times (2.5\sigma_{z1}/L)$, where r_1, r_2 are the singles proton rate for the two protons (3×10^7/s each), τ is the timing window (20 ns), σ_{z1} and σ_{z2} are the vertex resolution of the two protons (2 mm each) and L is the length of the target (40 cm). For 4 GeV positrons the two-proton accidental rate is 2800/s. If the quasi-elastic scattered positron is detected in the SBS in vertex and time anti-coincidence (veto) with the two-protons and has an efficiency of 99.9%, the background rate is then 3/s and it implies a signal-to-background ratio of 10^{-2} for 4 GeV positrons. The signal-to-background ratio for 2, 4 and 6 GeV positrons is shown in Fig. 13 over the Q^2 range that can be covered at each beam energy. The signal-to-background ratio falls off rapidly at lower Q^2 because of the reduced acceptance for forward angle positrons. The cut-off at high Q^2 comes from the limit on the detected proton momentum of < 500 MeV/c. As seen in Fig. 13, a significant range in Q^2 (0.08 - 0.25 GeV^2) can be covered at the three beam energies with signal-to-background ratio better than 1×10^{-2}. This range can be expanded to 0.025 GeV^2 by allowing a slightly worse signal-to-background ratio of 5×10^{-3}.

The next largest background is from quasi-elastic knockout of neutron followed by a charge exchange re-scattering. The angular range of interest (70 – 90 deg) corresponds to parallel kinematics for the quasi-elastic process and the rescattering cross section is at least an order of magnitude smaller [31]. Therefore this background is < 0.3/s and the signal-to-background for this process is better than 0.1.

Finally another background which is of concern is the the single pion production from deuterium ($\gamma^* + \mathrm{D} \rightarrow \mathrm{p} + \mathrm{p} + \pi^-$). The rates for these were estimated using the measured cross section for photoproduction of π^- from deuterium. The protons produced in this process are dominantly forward going in the lab. Therefore the rates for a pair of transverse protons from this process is several orders of magnitude lower compared to the other two backgrounds. However, this background could contribute to the background asymmetry because of the observed few % single spin asymmetry of in-elastic semi-inclusive pion production. This background asymmetry will have to be measured using the strategy discussed below. Further, since the asymmetry has a azimuthal angle dependence, it can be sampled by monitoring the azimuthal modulation of the background.

The positron capture process occurs only for negative helicity positrons and hence there is a large capture

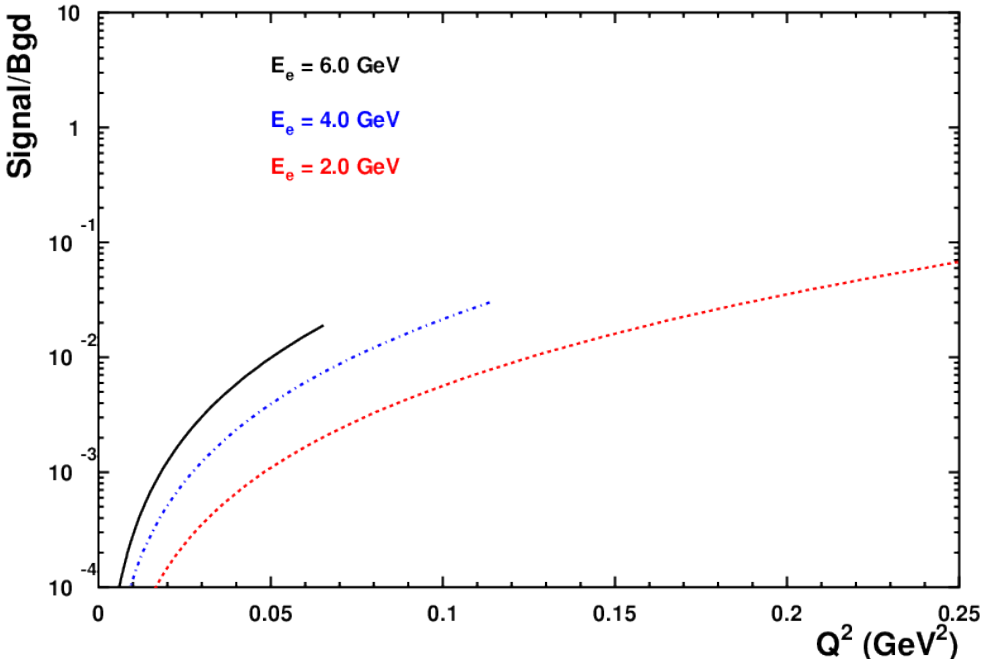

FIG. 13. Signal-to-background ratio for 2, 4 and 6 GeV positrons.

asymmetry which will be used as another means for isolating the capture signal (first discussed in Ref. [32, 33]). If we denote the total events for positive (negative) helicity positrons as $N^{\pm}$, with the capture signal as N_S and the background events as $N^{\pm}_{bgd}$, this gives $N^- = N_S + N^-_{bgd}$ and $N^+ = 0 + N^+_{bgd}$, which gives $N^- - N^+ = (N_S + < N_{bgd} > P_b A_{bgd})$, where P_b is the beam polarization and A_{bgd} is the background asymmetry. The strategy for measuring the background asymmetry is as follows; the asymmetry of the proton pairs detected at angles that are smaller and larger than the transverse signal protons will be measured. Assuming that the background asymmetry has a smooth angular variation, it will be extrapolated to the 70 - 90 degree range to obtain the true background asymmetry. Therefore, the background asymmetry can be measured simultaneously with the capture asymmetry (the signal). The measured asymmetry is;

$$A_{meas} = P_b \left(A_{capture} + A_{bgd}\right), \quad \text{with} \quad A_{capture} = \frac{N_S}{2 < N_{bgd} >}$$

For 4 GeV positrons the $A_{capture}$ is estimated to be 0.7%. We aim to measure the capture asymmetry with a statistical precision of 3%, which implies that the background asymmetry must be measured with an uncertainty of $\Delta A = 1/\sqrt{2N_{bg}} \sim 200$ ppm. False asymmetries, such as the beam charge asymmetry, must also be controlled at the same level. This requirement for the positron beam is many orders of magnitude less stringent compared to the requirements for "parity-quality" electron beams at JLab.

V. BEAM TIME REQUIREMENTS AND PROJECTIONS

In order to measure the capture asymmetry with 3% precision and the background asymmetry to better than ∼200 parts-per-million (ppm) for each beam energy, it requires about ∼20 days of beam with 200 nA current and 60% polarization. To perform this experiment at 3 different beam energies will need ∼ 60 days of beam time– a reasonable number given the physics reach of this experiment. Given the large electromagnetic backgrounds the higher polarization is better for the control of systematic uncertainties and the figure-of-merit does not improve with higher currents at the expense of beam polarization. The projected statistical precision for the extraction of the axial form factor for 60 days of beam time is shown in Fig. 14. A complete Geant4 simulation of the experiment is being developed which will be used to make more precise

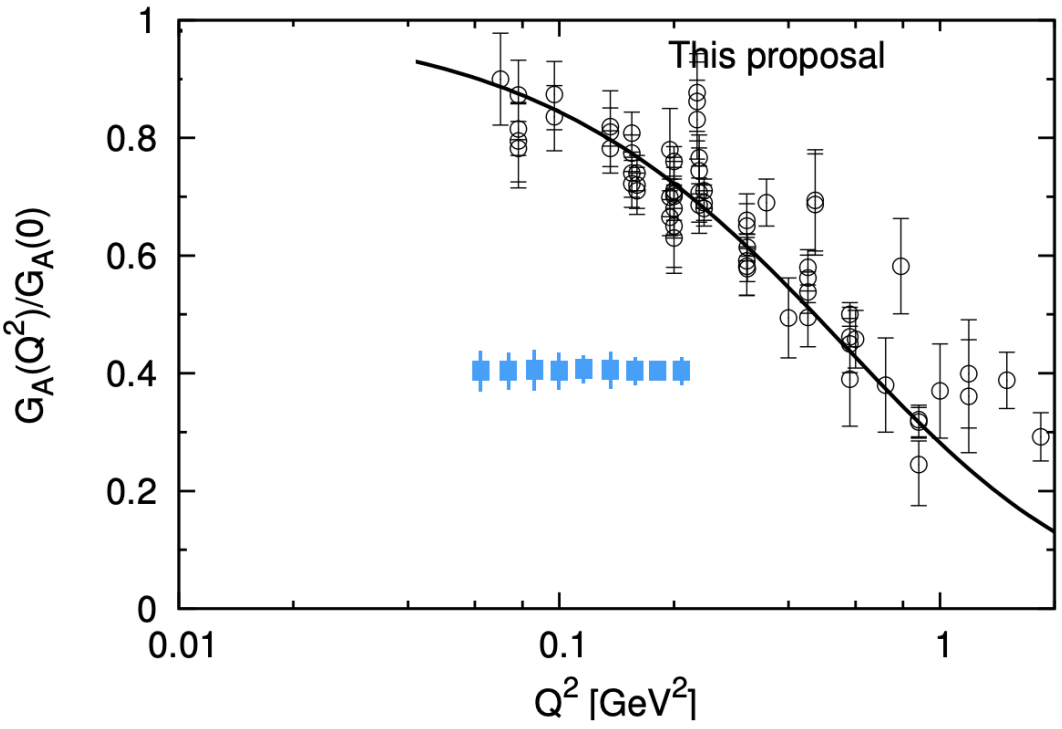

FIG. 14. The projected extraction of the axial form factor in the Q^2 range of 0.08 - 0.25 GeV^2, for 60 days of beam.

estimates of the signal and background and also the systematic uncertainty of this experiment.

VI. SUMMARY

The weak capture of positrons in ^2H with a medium energy (2 – 6 GeV), polarized (60%) positron beam at JLab, can be used to perform a new and unique measurement of the Q^2 dependence of $G_A(Q^2)$, the weak axial coupling g_A and the axial charge radius. These measurements would use recoil proton detection techniques that have been or are currently being developed for several experiments at JLab. The positron capture based measurement would have a completely different set of systematic uncertainties compared to all known methods and may help resolve several current puzzles. The experiment is feasible with modest requirements on the beam properties (60% polarization, 200 nA current and better than 200 ppm false asymmetry) and a modest amount of beam time.

[1] V. Punjabi, C. F. Perdrisat, M. K. Jones, E. J. Brash, and C. E. Carlson, Eur. Phys. J. A **51**, 79 (2015).
[2] D. Androic *et al.*, Nature **557**, 207 (2018).
[3] J. Gasser and H. Leutwyler, Ann. Phys. **158** (1984).
[4] V. Koch, LBNL-Report **38000** (1995), nucl-th:9512029.
[5] A. S. Meyer, M. Betancourt, R. Gran, and R. J. Hill, Phys. Rev. D **93**, 113015 (2016).
[6] S. Choi *et al.*, Phys. Rev. Lett. **71**, 3927 (1993).
[7] V. A. Andreev *et al.*, Phys. Rev. Lett. **99**, 032002 (2007).
[8] V. Bernard, L. Elouadrhiri, and U.-G. Meiß ner, J. Phys. G **28**, R1 (2002).
[9] H. Abele, Prog. Part. Nucl. Phys. **60**, 1 (2008).
[10] D. Dubbers and M. G. Schmidt, Rev. Mod. Phys. **83**, 1111 (2011).
[11] Particle Data Group, P. A. Zyla, *et al.*, Prog Theor Exp Phys **2020**, 10.1093/ptep/ptaa104 (2020).
[12] R. L. Workman *et al.*, Prog. Theo. Exp. Phys. **2022**, 083C01 (2022).

[13] A. Czarnecki, W. J. Marciano, and A. Sirlin, Phys. Rev. Lett. **120**, 202002 (2018).
[14] UCNA Collaboration, M. A.-P. Brown, *et al.*, Phys. Rev. C **97**, 035505 (2018).
[15] N. Fomin, Private Communication (2023).
[16] W. J. Marciano and A. Sirlin, Phys. Rev. Lett. **96**, 032002 (2006).
[17] A. Czarnecki, W. J. Marciano, and A. Sirlin, Phys. Rev. Lett. **120**, 202002 (2018).
[18] G. L. Greene and P. Geltenbort, Sci. Am. **314**, 36 (2016).
[19] F. M. Gonzalez *et al.*, Phys. Rev. Lett. **127**, 162501 (2021).
[20] J. C. Hardy and I. S. Towner, Phys. Rev. C **91**, 025501 (2015).
[21] A. A. Aguilar-Arevalo *et al.* (MiniBooNE Collaboration), Phys. Rev. D **81**, 092005 (2010).
[22] V. Lyubushkin *et al.*, Eur. Phys. J. C **63**, 355–381 (2009).
[23] U. Mosel and O. Lalakulich, Nuclear Physics News **29** (2012).
[24] A. S. Meyer, A. Walker-Loud, and C. Wilkinson, Ann. Rev. Nucl. Part. Sci. **72**, 205 (2022), arXiv:2201.01839 [hep-lat].
[25] T. Cai *et al.*, Nature **614**, 48 (2023).
[26] H. Primakov, Muon physics (Academic, New York, 1975) p. 3.
[27] K. Kubodera, J. Delorme, and M. Rho, Phys. Rev. Lett. **40**, 755 (1978).
[28] M. Ding, C. D. Roberts, and S. M. Schmidt, Particles **6** (2023), arXiv:2211.07763.
[29] W.-Y. P. Hwang, Phys. Rev. C **33**, 1370 (1986).
[30] S. L. Mintz, M. A. Barnett, and G. M. Gerstner, Int. J. Mod. Phys. E **6**, 111 (1996).
[31] C. Barbieri, L. Lapikas, and D. Rohe, Eur. Phys. J. A **24**, 85 (2005).
[32] A. Deur, JLab LOI **04-006** to PAC 25 (2004).
[33] A. Deur, AIP Conf. Proc. **1563** (2013), arXiv:1307.2927.
[34] S. Kuhn *et al.*, Jlab experiment E**12-06-113:** the structure of the free neutron at large x-bjorken (2006).
[35] Z. A. Meziani *et al.*, Jlab experiment E**12-17-012:** partonic structure of light nuclei (2015).
[36] C. Keppel, B. Wotsekhowski, P. King, D. Dutta, N. Liyanage, R. Montgomery, *et al.*, Jlab experiment C**12-15-006:** measurement of tagged deep inelastic scattering (2015).